Received: 19 February 2024 | Revised: 7 June 2024 | Accepted: 9 July 2024

DOI: 10.1111/bph.17318

RESEARCH ARTICLE

Schwann cell transient receptor potential ankyrin 1 (TRPA1) ortholog in zebrafish larvae mediates chemotherapy-induced peripheral neuropathy

Elisa Bellantoni[1] | Matilde Marini[1] | Martina Chieca[1] | Chiara Gabellini[2] | Erica Lucia Crapanzano[2] | Daniel Souza Monteiro de Araujo[1] | Daniele Nosi[3] | Lorenzo Roschi[4] | Lorenzo Landini[1] | Gaetano De Siena[1] | Pasquale Pensieri[1] | Alessandra Mastricci[1] | Irene Scuffi[1] | Pierangelo Geppetti[1,5,6] | Romina Nassini[1] | Francesco De Logu[1]

[1]Department of Health Sciences, Clinical Pharmacology and Oncology Section, University of Florence, Florence, Italy

[2]Department of Biology, Unit of Cell and Developmental Biology, University of Pisa, Pisa, Italy

[3]Department of Experimental and Clinical Medicine, University of Florence, Florence, Italy

[4]LENS—European Laboratory for Nonlinear Spectroscopy, University of Florence, Florence, Italy

[5]Department of Molecular Pathobiology, College of Dentistry, New York University, New York, New York, USA

[6]Pain Research Center, College of Dentistry, New York University, New York, New York, USA

Correspondence
Romina Nassini, Department of Health Sciences, Clinical Pharmacology and Oncology Section, University of Florence, Florence 50139, Italy.
Email: romina.nassini@unifi.it

Funding information
Fondazione Cassa di Risparmio di Firenze–Human Brain Optical Mapping Project; Fondazione Telethon, Grant/Award Number: GMR22T1070; European Union—Next Generation EU, National Recovery and Resilience Plan, Mission 4 Component 2—

Abstract

Background and Purpose: The oxidant sensor transient receptor potential ankyrin 1 (TRPA1) channel expressed by Schwann cells (SCs) has recently been implicated in several models of neuropathic pain in rodents. Here we investigate whether the pro-algesic function of Schwann cell TRPA1 is not limited to mammals by exploring the role of TRPA1 in a model of chemotherapy-induced peripheral neuropathy (CIPN) in zebrafish larvae.

Experimental Approach: We used zebrafish larvae and a mouse model to test oxaliplatin-evoked nociceptive behaviours. We also performed a TRPA1 selective silencing in Schwann cells both in zebrafish larvae and mice to study their contribution in oxaliplatin-induced CIPN model.

Key Results: We found that zebrafish larvae and zebrafish TRPA1 (zTRPA1)-transfected HEK293T cells respond to reactive oxygen species (ROS) with nociceptive behaviours and intracellular calcium increases, respectively. TRPA1 was found to be co-expressed with the Schwann cell marker, SOX10, in zebrafish larvae. Oxaliplatin caused nociceptive behaviours in zebrafish larvae that were attenuated by a TRPA1 antagonist and a ROS scavenger. Oxaliplatin failed to produce mechanical allodynia in mice with Schwann cell TRPA1 selective silencing (*Plp1*$^{+}$-*Trpa1* mice). Comparable results were observed in zebrafish larvae where TRPA1 selective silencing in Schwann cells, using the specific Schwann cell promoter myelin basic protein (MBP), attenuated oxaliplatin-evoked nociceptive behaviours.

Abbreviations: CIPN, chemotherapy-induced peripheral neuropathy; HEK293T, human embryonic kidney; PLP1, proteolipid protein 1; ROS, reactive oxygen species; SC, Schwann cell.

Elisa Bellantoni, Matilde Marini and Martina Chieca have contributed equally to this work.

Investment 1.4—National Center for Gene Therapy and Drugs based on RNA Technology, Grant/Award Number: CUP B13C22001010001; European Union—Next Generation EU, National Recovery and Resilience Plan, Mission 4 Component 2—Investment 1.3—Mnesys A multiscale integrated approach to the study of the nervous system in health and disease, Grant/Award Number: CUP B83C22004910002

Conclusion and Implications: These results indicate that the contribution of the oxidative stress/Schwann cell/TRPA1 pro-allodynic pathway to neuropathic pain models seems to be conserved across the animal kingdom.

KEYWORDS
nociceptive behaviours, oxaliplatin, oxidative stress, Schwann cells, transient receptor potential ankyrin 1 (TRPA1)

1 | INTRODUCTION

Zebrafish represent an alternative and informative model for the study of pain and its treatment (Malafoglia et al., 2013; Ohnesorge et al., 2021). Growing evidence shows that zebrafish modulate their behaviour in response to mechanical, chemical or thermal painful stimuli (Curtright et al., 2015) by two different populations of somatosensory neurons in the head and body, trigeminal neurons and Rohon–Beard (RB) neurons, respectively (Prober et al., 2008). Zebrafish larvae exhibit effortless evaluable pain behaviours and specifically allow the study of the pathophysiology and pharmacology of unmyelinated axons, as Rohon-Beard (RB) neurons are typically unmyelinated (Koudelka et al., 2016; Lysko & Talbot, 2022).

A member of the **transient receptor potential (TRP) family** of channels, the ankyrin 1 subtype (**TRPA1**), has been implicated in various pain models (Nassini et al., 2014; Souza Monteiro de Araujo et al., 2020). TRPA1 is highly sensitive to oxidative stress and amplifies reactive oxygen species (ROS) production (De Logu et al., 2017; De Logu, Souza Monteiro de Araujo, et al., 2021; Takahashi & Mori, 2011). Zebrafish express two TRPA1 paralogs (TRPA1a and TRPA1b) (Prober et al., 2008). TRPA1a is exclusively expressed in most posterior vagal ganglion neurons, which innervate various visceral organs, including the gut, whereas TRPA1b is mainly expressed in a subset of trigeminal and RB sensory neurons that innervate skin and other somatic tissues (Prober et al., 2008). *In vivo* and *in vitro* studies suggest that TRPA1b is the major contributor to chemical sensation deriving from both internal and external stimuli, whereas TRPA1a function is limited to internal stimuli (Prober et al., 2008).

Chemotherapy-induced peripheral neuropathy (CIPN) is one of the most frequent and disabling side effects of several anticancer drugs, including platinum-based drugs (Banach et al., 2017; Zajaczkowska et al., 2019), which occurs in approximatively 90% of patients receiving chemotherapy (Fallon, 2013). CIPN symptoms are varied in duration and intensity from acute, thermal and tactile allodynia or hyperalgesia to chronic pain and irreversible nerve damage (Seretny et al., 2014; Zajaczkowska et al., 2019). The mechanisms underlying painful CIPN are poorly understood. In recent years, zebrafish have gained prominence as a preclinical drug discovery model thanks to many advantages, including the large number of larvae available, whole immunohistochemistry imaging and the conservation of 80% of human disease-causing genes (Goldsmith & Jobin, 2012). CIPN models in zebrafish show marked similarity to mammal models (Cirrincione & Rieger, 2020). A dose-dependent reduction in sensory axon branch density and altered movement was reported in zebrafish embryos treated with **vincristine** and **bortezomib** (Khan et al., 2012). **Paclitaxel** treatment in zebrafish larvae induces degeneration of unmyelinated axons of RB sensory neurons and increases sensitivity to mechanical stress and hydrogen peroxide levels (Lisse et al., 2016). We previously reported the implication of TRPA1 and TRP vanilloid 4 (**TRPV4**) and oxidative stress, in mediating mechanical and cold hypersensitivity in different mouse models of CIPN (De Logu et al., 2020; Materazzi et al., 2012; Nassini et al., 2011; Trevisan et al., 2013). More recently, antagonism of sigma-1 receptor reduced the trafficking of TRPA1 to the plasma membrane preventing the painful symptoms associated with CIPN in mice (Marcotti et al., 2023).

Schwann cells (SCs), among the most represented nucleated cells of peripheral nerves, are known to protect and nurture nerve fibres (Oliveira et al., 2023). Recently, we reported in mouse models of neuropathic, cancer and migraine pain a novel pro-algesic function of SCs that, via TRPA1, sense and amplify oxidative stress burden to signal mechanical allodynia to adjacent nerve fibres (De Logu et al., 2020, 2017; De Logu et al., 2023; De Logu, Marini, et al., 2021; Landini

What is already known

- The TRPA1 channel in Schwann cells is linked to neuropathic pain in rodent models.

What does this study add

- The oxidative stress/Schwann cell/TRPA1 pathway contribution to neuropathic pain is conserved across different species.

What is the clinical significance

- Zebrafish provides an *in vivo* model for studying Schwann cells/TRPA1/oxidative stress in pain responses.
- TRPA1 is a potential target for therapeutic intervention in neuropathic pain across various models.

et al., 2022). Here, we asked whether the SC/TRPA1/oxidative stress pathway plays a role in producing and sustaining pain-like response in Zebrafish. By using *in vitro* biochemical assay and *in vivo* behavioural and genetic techniques, we found that zebrafish TRPA1 (zTRPA1) in zebrafish SCs behaves as an oxidative stress sensor and amplifier, thus contributing to the algesic symptoms of CIPN evoked by **oxaliplatin**, as observed in mice.

2 | METHODS

2.1 | Animals

All animal studies are reported in compliance with the ARRIVE guidelines (Percie du Sert et al., 2020a) and with the recommendations made by the British Journal of Pharmacology (Lilley et al., 2020).

2.1.1 | Zebrafish (*Danio rerio*)

Wild-type zebrafish larvae of the WT AB line and Casper (nacre$^{w2/w2}$ and roy$^{a9/a9}$) zebrafish larvae were used for all behavioural experiments. Animals were handled in compliance with protocols approved by the Italian Ministry of Public Health and the local Ethical Committee of the University of Pisa (authorization #1695-2023), in conformity with EU legislation (Directive 2010/63/EU). Adult and larval zebrafish were maintained on a 14/10 h light/dark cycle at 28.5°C. Embryos were raised in E3 medium (5 mM NaCl, 0.17 mM KCl, 0.33 mM $CaCl_2$, 0.33 mM $MgSO_4$) containing 0.00016% methylene blue (Kimmel et al., 1995).

2.1.2 | Mice

To generate mice in which the *Trpa1* gene was conditionally silenced in SCs, homozygous 129S-Trpa1tm2Kykw/J (floxed Trpa1, Trpa1fl/fl, RRID:IMSR_JAX:008649; Jackson Laboratory) were crossed with hemizygous B6.CgTg (Plp1-CreERT)3Pop/J mice (Plp1-CreERT, RRID:IMSR_JAX:005975; Jackson Laboratory), expressing a tamoxifen-inducible Cre in their SCs (proteolipid protein myelin 1 [Plp1]) (De Logu et al., 2017). The progeny (*Plp1-Cre^{ERT};Trpa1$^{fl/fl}$*) was genotyped using PCR for Trpa1 and Plp1-Cre^{ERT}. Mice that were negative for Plp1-Cre^{ERT} (*Plp1-Cre^{ERT-};Trpa1$^{fl/fl}$*) were used as control. Both positive and negative mice for Cre^{ERT} and homozygous floxed Trpa1 (*Plp1^{+}-Trpa1* and control, respectively, male 25–30 g, 6–8 weeks old) were treated with intraperitoneal (i.p.) **4-hydroxytamoxifen (4-OHT**, 1 mg 100 µl^{-1} in corn oil once a day consecutively for 3 days). To selectively delete *Trpa1* in primary sensory neurons, homozygous 129S-Trpa1$^{tm2Kykw/J}$ (floxed Trpa1, *Trpa1$^{fl/fl}$*, RRID:IMSR_JAX:008649; Jackson Laboratory) mice were crossed with hemizygous Advillin-Cre mice (Adv-Cre). Mice positive or negative for Cre and homozygous for floxed Trpa1 (*Adv-Trpa1* and control, respectively) were used. The successful Cre-driven deletion of TRPA1 mRNA was confirmed using reverse transcription quantitative real-time PCR (RT-qPCR). The group size of n = 8 mice for behavioural experiments was determined by sample size estimation using G*Power (v3.1; Faul et al., 2007) to detect the size effect in a post hoc test with types 1 and 2 error rates of 5% and 20%, respectively. Allocation concealment of mice into the vehicle(s) or treatment groups was performed using a randomization procedure (http://www.randomizer.org/). The assessors were blinded to the identity of the animals (genetic background) or allocation to treatment groups. None of the animals were excluded from the study. Animal experiments and sample collections were carried out according to the European Union (EU) guidelines for animal care procedures and Italian legislation (DLgs 26/2014) application of the EU Directive 2010/63/EU. All animal studies were approved by the Animal Ethics Committee of the University of Florence and the Italian Ministry of Health (#1194/2015-PR). Animals were anaesthetized with a mixture of ketamine and **xylazine** (90 and 3 mg·kg^{-1}, respectively, i.p.) and killed with inhaled CO_2 plus 10% to 50% O_2. Confirmation of death was achieved by a physical method of killing (decapitation). Mice were housed in a temperature (20 ± 2°C) and humidity (50% ± 10%) controlled *vivarium* (12 h dark/light cycle, free access to food and water, five animals per cage). At least 1 h before behavioural experiments, mice were acclimatized to the experimental room and behaviour was evaluated between 9:00 AM and 5:00 PM. All the procedures were conducted following the current guidelines for laboratory animal care and the ethical guidelines for investigations of experimental pain in conscious animals set by the International Association for the Study of Pain (Zimmermann, 1983).

2.2 | Behavioural analysis

2.2.1 | Locomotor tracking assay

Five days post fertilization (dpf) zebrafish larvae were placed in 200 µl of E3 medium in a 96-well plate. For each experimental condition, a group of at least eight larvae were used. Larvae were acclimated to the wells for 600 s, after which an eight-channel pipette was used to simultaneously dispense 200 µl of 2× concentration of the TRPA1 agonists in E3 medium into each well (final concentration: **allyl isothiocyanate [AITC**, 0.01–0.1–1–10 µM], **4-hydroxynonenal [4-HNE**, 1–10–100 µM] and **hydrogen peroxide [H_2O_2**, 100–1000 µM]). Locomotor activity was subsequently tracked with EthoVision® XT (Version 17, Noldus) and quantified as cumulative distance moved in mm/0.05 s. For incubation with TRPA1 antagonist **A-967079**, larvae were placed in a 96-well plate pretreated with A-967079 (10 µM) in 200 µl E3 medium for 10 min. After incubation, 200 µl of 2× concentration of TRPA1 agonist was added directly to the well, and the resulting behaviour was recorded. In another set of experiments, larvae were placed in a Petri dish loaded with oxaliplatin (1–10 µM) in E3 medium for 4 days, from 1 to 5 dpf, and t locomotor activity was tracked at 5 days post fertilization. Some larvae were co-incubated with **glutathione (GSH**, 10 µM) and oxaliplatin or vehicle.

2.2.2 | Acute nociceptive behaviour

Zebrafish larvae at 24–27 h post fertilization (hpf) were manually dechorionated and acclimated for 10 s in 12-well plates. Larvae were stimulated with 2× concentration of AITC (50–100–500 μM), 4-HNE (100–500–1000 μM) and H_2O_2 (30–100–300 mM) in E3 medium. Immediately after stimulation, the number of writhing movements (tail coils) in a range of 10 s was counted. Single writhes were counted when the tail was coiled either to the left or right of the embryo. Some larvae were exposed to A-967079 (30 μM) for 10 min before exposure to TRPA1 agonists.

2.2.3 | Light touch response

Zebrafish larvae at 24–27 post fertilization were manually dechorionated, and touch-evoked behaviours were elicited by striking the tail of the larvae with a sideways motion up to three times using a dulled 0.2 mm insect pin attached to a surgical blade holder. A response was considered positive when writhing behaviour was observed immediately after tactile stimulus. To avoid any pre-stimulus modulation of the response, we waited about 5 s between each stimulus. Larvae were exposed to AITC (50–100–500 μM), 4-HNE (100–500–1000 μM) and H_2O_2 (30–100–300 mM) individually in 12-well plates for 3 min, after which tactile stimulus was applied. Some larvae were exposed to A-967079 (30 μM) for 10 min before exposure to TRPA1 agonists for 3 min before the test.

2.2.4 | Mechanical allodynia

The mechanical paw-withdrawal threshold was measured in mice using von Frey filaments of increasing stiffness (0.02–2 g) applied to the plantar surface of the mouse hind paw, according to the up-and-down paradigm (Chaplan et al., 1994). The 50% mechanical paw-withdrawal threshold (g) response was then calculated from the resulting scores. Mechanical paw-withdrawal threshold was measured at baseline and at different times following treatments.

2.3 | Immunofluorescence

The Immuno-related procedures used comply with the recommendations made by the *British Journal of Pharmacology* (Alexander et al., 2018).

2.3.1 | Whole-mount immunofluorescence in zebrafish larvae

Five days post fertilization zebrafish larvae were anesthetized in 0.016% tricaine and fixed in 4% paraformaldehyde overnight at 4°C. After fixation, zebrafish larvae were washed three times in PBS + 0.3% Triton-X (PBT) for 5 min. Blocking was performed using normal donkey serum (5% NDS), dimethyl sulfoxide (10% DMSO) and 0.1% Tween-20 in phosphate buffer saline (PBS) for 1 h and incubated with the following primary antibodies: anti-acetylated tubulin (#T7451, mouse monoclonal, 1:500; Merck, RRID:AB_609894) and SOX10 (#GTX128374, rabbit polyclonal, 1:200; GeneTex, RRID:AB_2885766) diluted in blocking solution overnight at 4°C. Larvae were washed five times with PBT for 10 min, blocked with blocking solution for 1 h and incubated with the following fluorescent polyclonal secondary antibodies: Alexa Fluor® 488 (#A32731, goat polyclonal anti-mouse, 1:1000; Thermo Fisher Scientific, RRID:AB_2633280) and Alexa Fluor® 594 (#A21207, donkey polyclonal anti-rabbit, 1:1000; Thermo Fisher Scientific, RRID:AB_141637) diluted in the blocking solution for 2 h. After incubation with secondary antibody, larvae were washed with PBST three times for 10 min and coverslipped using water-based mounting medium containing **DAPI** (#ab104139, Abcam). Slides were visualized and analysed using a ZEISS Axio Imager 2 microscope with Z-stacks in the Aptome mode (ZEISS).

2.3.2 | Immunofluorescence in mouse sciatic nerves and dorsal root ganglion

Sciatic nerves were collected, postfixed for 24 h in 4% paraformaldehyde and cryoprotected in 30% sucrose until cryosectioning (10 μm). The slides were washed three times for 10 min and blocked with blocking solution 5% normal goat serum (NGS) for 1 h and incubated with 4-HNE primary antibody (#ab48506, mouse monoclonal, 1:25; Abcam, RRID:AB_867452) or TRPA1 (#ACC-037, rabbit polyclonal, 1:200; Alomone, RRID:AB_2040232; #NB110-40763, rabbit polyclonal, 1:200; Novus Biologicals, RRID:AB_715124) diluted in blocking solution for 1 h and washed two times for 10 min. Sections were then incubated with the fluorescent secondary antibodies Alexa Fluor® 594 (#A11005, goat polyclonal anti-mouse, 1:600; Thermo Fisher Scientific, RRID:AB_2534073), Alexa Fluor® 488 (#A32731, goat polyclonal anti-rabbit, 1:600; Thermo Fisher Scientific, RRID:AB_2633280) and Alexa Fluor® 594 (#A21207, donkey polyclonal anti-rabbit, Thermo Fisher Scientific, RRID:AB_141637) diluted in blocking solution for 2 h. After incubation with secondary antibody, the slides were washed two times for 10 min and slides containing 4-HNE antibody were coverslipped using the mounting medium with DAPI (#ab104139, Abcam); slides containing TRPA1 were incubated with S100 beta antibody (#ab196175, monoclonal anti-rabbit Alexa Fluor® 647, 1:50; Abcam, RRID:AB_2868562) or NeuN (#MAB377X, monoclonal anti-mouse Alexa Fluor® 488, 1:250; Merck, RRID:AB_2149209). Slides were again washed three times for 10 min and were coverslipped using the mounting medium with DAPI (#ab104139, Abcam). All slides were visualized and analysed using a ZEISS Axio Imager 2 microscope with Z-stacks in the Apotome mode (ZEISS). The 4-HNE staining was reported as the fluorescence intensity. Pearson correlation (Rcoloc) values in the colocalization analysis were calculated using the

colocalization Plugin of the ImageJ (v.1.54f; National Institutes of Health, Bethesda, MD, USA).

2.4 | Axon branch density analysis

Images of the lateral view of 5 days post fertilization zebrafish larvae, stained with anti-acetylated tubulin, were analysed with ImageJ Software (NIH, USA). The images were converted in 8 bits, and fluorescence intensity was calculated measuring the average of three different regions of interest (area: 10,000 μm^2) for each zebrafish larva. Data were reported as axon branch density/μm^2.

2.5 | Dual RNAScope Fluorescent in situ hybridization and immunofluorescence

Fluorescent *in situ* hybridization was performed using RNAscope™ Multiplex Fluorescent V2 Assay (ACDbio), according to manufacturer's protocol. Whole zebrafish larvae were fixed with paraformaldehyde 4% in PBS for 17–24 h at room temperature (RT). Larvae were washed with PBST for 10 min at RT and dehydrated in 25%, 50%, 75% and 100% methanol for 10 min. Larvae were incubated with 0.2 M HCl in 100% methanol at RT for 30 min and rehydrated by subsequent steps in 75%, 50% and 25% methanol at RT for 10 min. For targeting retrieval, larvae were incubated at 100°C with 1× Target Retrieval Solution (ACDbio) for 15 min and then incubated with Protease Plus (ACDbio) at 40°C for 1 h. Slides were incubated at 40°C in HybEZ II Oven (ACDbio) and hybridized for 2 h with probes to detect *TRPA1b* mRNA. Signal amplification was obtained by consecutive incubations with the 3 antimicrobial peptides, AMP1, AMP2 and AMP3 reagents and RNAscope Multiplex FL v2 HRP-C1 enzyme (ACDbio) for 15 min at 40°C. Then, larvae were incubated for 30 min at 40°C with fluorophore (#7534 TSA Vivid-520 ACDbio) for labelling the C1 probe. Any further HRP activity was stopped by incubation with HRP blocker for 15 min at 40°C. For immunohistochemistry, larvae were blocked in blocking solution (5% NDS, 10% DMSO, 0.1% Tween-20, PBS) for 2 h and incubated with primary antibodies:- SOX10 (#GTX128374, rabbit polyclonal, 1:200; GeneTex) and anti-acetylated tubulin (#T7451, mouse monoclonal, 1:500 Merck) diluted in the blocking solution overnight at 4°C. Larvae were washed five times with PBT for 10 min, blocked with blocking solution for 1 h and incubated with the following fluorescent polyclonal secondary antibodies: Alexa Fluor® 488 (#A32731, goat polyclonal anti-mouse, 1:1000; Thermo Fisher Scientific) and Alexa Fluor® 594 (#A21207, donkey polyclonal anti-rabbit, 1:1000; Thermo Fisher Scientific) diluted in the blocking solution for 2 h at RT and coverslipped using the mounting medium with DAPI. All slides were visualized and analysed using a confocal microscope Stellaris 5 (Leica). The percentage of TRPA1b positive SOX10 nuclei was counted (10^4 μm^2 images) in the whole-mount zebrafish larvae at 5 days post fertilization.

2.6 | Cell line

2.6.1 | Human embryonic kidney 293T (HEK293T)

HEK293T cells (#CRL-3216, RRID:CVCL_0063; ATCC) were maintained in Dulbecco's modified Eagle's medium (DMEM) high glucose supplemented with 10% heat inactivated fetal bovine serum (FBS), 2 mM L-glutamine and 1 mM penicillin/streptomycin at 37°C in 5% CO_2 and 95% O_2.

2.6.2 | Cell transfection

HEK293T cells were plated on poly-L-lysine-coated (8.3 μM) 35 mm glass coverslips and maintained at 37°C in 5% CO_2 and 95% O_2 16 h before transfection; then, cells were transfected with plasmid DNA (1 μg) expressing TRPA1b gene (pcDNA3.1-zTRPA1b, kindly donated by Prof Richard M. van Rijn, Purdue University College of Pharmacy, West Lafayette, USA) using polyethylenimine in a ratio of 1:3 (#23966, PEI, Polyscience).

2.7 | Calcium imaging

Cells were plated on poly-L-lysine-coated (8.3 μM) 35 mm glass coverslips and maintained at 37°C in 5% CO_2 and 95% O_2 for 24 h. Cells were loaded for 40 min with Fura-2, AM ester (5 μM) added to the buffer solution (37°C) containing (in mM) 2 $CaCl_2$; 5.4 KCl; 0.4 $MgSO_4$; 135 NaCl, 10 D-glucose, 10 HEPES and 0.1% bovine serum albumin (BSA). Cells were washed and transferred to a chamber on the stage of a fluorescent microscope for recording (Axio Observer 7; with a fast filter wheel and Digi-4 lens to record excitations ZEISS). Cells were exposed to AITC (10 nM to 100 μM), H_2O_2 (10 μM to 1 mM) or 4-HNE (1–100 μM), and the calcium response was monitored in the presence of A-967079 (30 μM, 10 min of incubation) or its vehicle (0.001% DMSO). In another set of experiments, zTRPA1b transfected cells were first stimulated with oxaliplatin (300 μM) for 10 min and then with a subthreshold concentration of H_2O_2 (30 μM), also in the presence of A-967079 (30 μM) or GSH reduced (30 μM). Results were expressed as percentage increase in ratio 340/380 over baseline normalized to the maximum effect induced by ionomycin (5 μM) added at the end of each experiment.

2.8 | H_2O_2 assay

H_2O_2 levels were assessed in zebrafish larvae homogenates using the Amplex Red® assay (Invitrogen, Waltham, MA, USA), according to the manufacturer's protocol. Fluorescence excitation and emission were measured at 540 and 590 nm, respectively. H_2O_2 production was calculated using the H_2O_2 standard and expressed as nmol·mg^{-1} protein.

2.9 | Plasmid construction

pTST3-Hyper7 was produced using Gibson assembly strategy (Gibson Assembly® Master Mix NEB #E2611L) starting from pT3TS-RfxCas13d-HA (RRID: Addgene #141320) backbone (P1/P2) and Hyper7 coding sequence (P3/P4) kindly donated by Emrah Eroglu (Pak et al., 2020). pTST3-Tol2 was produced using Gibson assembly strategy starting from pT3TS-RfxCas13d-HA backbone (P5/P6), and Tol2 coding sequence was amplified from pRP[Exp]-CAG>Tol2 transposase (P7/P8) (VectorBuilder). All constructs were confirmed by Sanger sequencing. All primer (P) sequences are reported in Table S1.

2.10 | Microinjection

Hyper7 and Tol2 mRNAs were *in vitro* transcribed with T3 promoter using mMESSAGE mMACHINE™ T3 Transcription Kit (Thermo Fisher #AM1348). Hyper7 mRNA was injected (300 pg per embryo) into the yolk of one-cell-stage zebrafish embryos using a microinjector (Narishige, Japan). pTol2[miR30]-(Gow et al.)>TurboGFP-dre_trpa1b [miR30-shRNA#1] (trpa1b shRNA 5′-ATCATCTACATTGCACAT-TAAT-3′) from VectorBuilder was linearized using ApaLI restriction enzyme (NEB #R0507S). Then, linearized plasmid (25 pg per embryo) was injected into the zygote of one-cell-stage zebrafish embryos in the presence of Transposase Tol2 mRNA (100 pg per embryo) to be integrated in the zebrafish embryo genome.

2.11 | Statistical analysis

The data and statistical analysis comply with the recommendations on experimental design and analysis in pharmacology (Curtis et al., 2022). The results are expressed as the mean ± SEM. For multiple comparisons, a one-way ANOVA followed by a post hoc Bonferroni's test was used. The two groups were compared using Student's *t* test. For mouse behavioural experiments with repeated measures, a two-way mixed-model ANOVA followed by a post hoc Bonferroni's test was used. Statistical analyses were performed on raw data using GraphPad Prism 8 (GraphPad Software Inc.). Before statistical significance analysis was performed, data were tested for normality using the Kolmogorov–Smirnov test and homogeneity using the Bartlett test. *P* values less than 0.05 ($P < 0.05$) were considered significant. EC_{50} values were determined from non-linear regression models using Graph Pad Prism 8. The statistical tests used and sample size for each analysis are shown in the figure legends.

2.12 | Materials

If not otherwise indicated, all reagents were from Merck Life Science S.r.l. (Milan, Italy). Details of other materials and suppliers were provided in the specific sections.

2.13 | Nomenclature of targets and ligands

Key protein targets and ligands in this article are hyperlinked to corresponding entries in the IUPHAR/BPS Guide to PHARMACOLOGY http://www.guidetopharmacology.org and are permanently archived in the Concise Guide to PHARMACOLOGY 2023/2024 (Alexander, Christopoulos, et al., 2023; Alexander, Mathie, et al., 2023).

3 | RESULTS

3.1 | TRPA1 agonists induce nociceptive-like behaviour in zebrafish larvae

Two TRPA1 paralogs (TRPA1a and TRPA1b) are expressed in zebrafish and are activated by AITC and 4-HNE (Prober et al., 2008) that are known pain-inducing molecules and TRPA1 agonists in mammals (Jordt et al., 2004; Trevisani et al., 2007). However, only TRPA1b is sensitive if compounds are applied as external stimuli (Prober et al., 2008). First, we confirmed that AITC and 4-HNE concentration dependently increases intracellular calcium in zTRPA1b-HEK293T cells, a response that was inhibited by the selective TRPA1 antagonist A-967079 (Figure 1a,b). Intraplantar administration of AITC and 4-HNE in the mouse hindpaw is known to evoke early and transient spontaneous nociceptive behaviours (Trevisani et al., 2007) that are followed by a delayed and sustained mechanical allodynia (De Logu et al., 2023). As previously reported (Ko et al., 2019; Prober et al., 2008; Stevens et al., 2018) in zebrafish larvae (5 days post fertilization), AITC (0.01–0.1–1–10 μM) and 4-HNE (1–10–100 μM) dose dependently and transiently (300 s) increased the locomotor activity (Figure 1c,d), a behavioural pain-like response that was inhibited by A-967079 (Figure 1e,f). Also, larvae at early stages of development (24–27 post fertilization), exposed to AITC (50–100–500 μM) and 4-HNE (100–500–1000 μM), responded with a dose-dependent and transient enhancement in the number of tail coils. The response was attenuated by pretreatment with A-967079 (Figure 1g,h). Zebrafish larvae (24–27 post fertilization) exposed to AITC or 4-HNE also showed enhanced responsivity to light tactile stimuli (Figure 1i,j), which is considered a reliable index of mechanical sensitization (Faucherre et al., 2013; Low et al., 2010; Pietri et al., 2009). This response was abated in the presence of A-967079 (Figure 1i,j). These data support the hypothesis that the zebrafish model recapitulates TRPA1 functions described in mammals, as the channel appears to mediate transient noxious sensations and sustained mechanical hypersensitivity.

3.2 | zTRPA1 encodes the response to oxidative stress

TRPA1 channel is activated by multiple oxidative stress agents including H_2O_2 (Andersson et al., 2008; Landini et al., 2022; Nassini et al., 2014; Sawada et al., 2008). *In vitro* experiments showed that

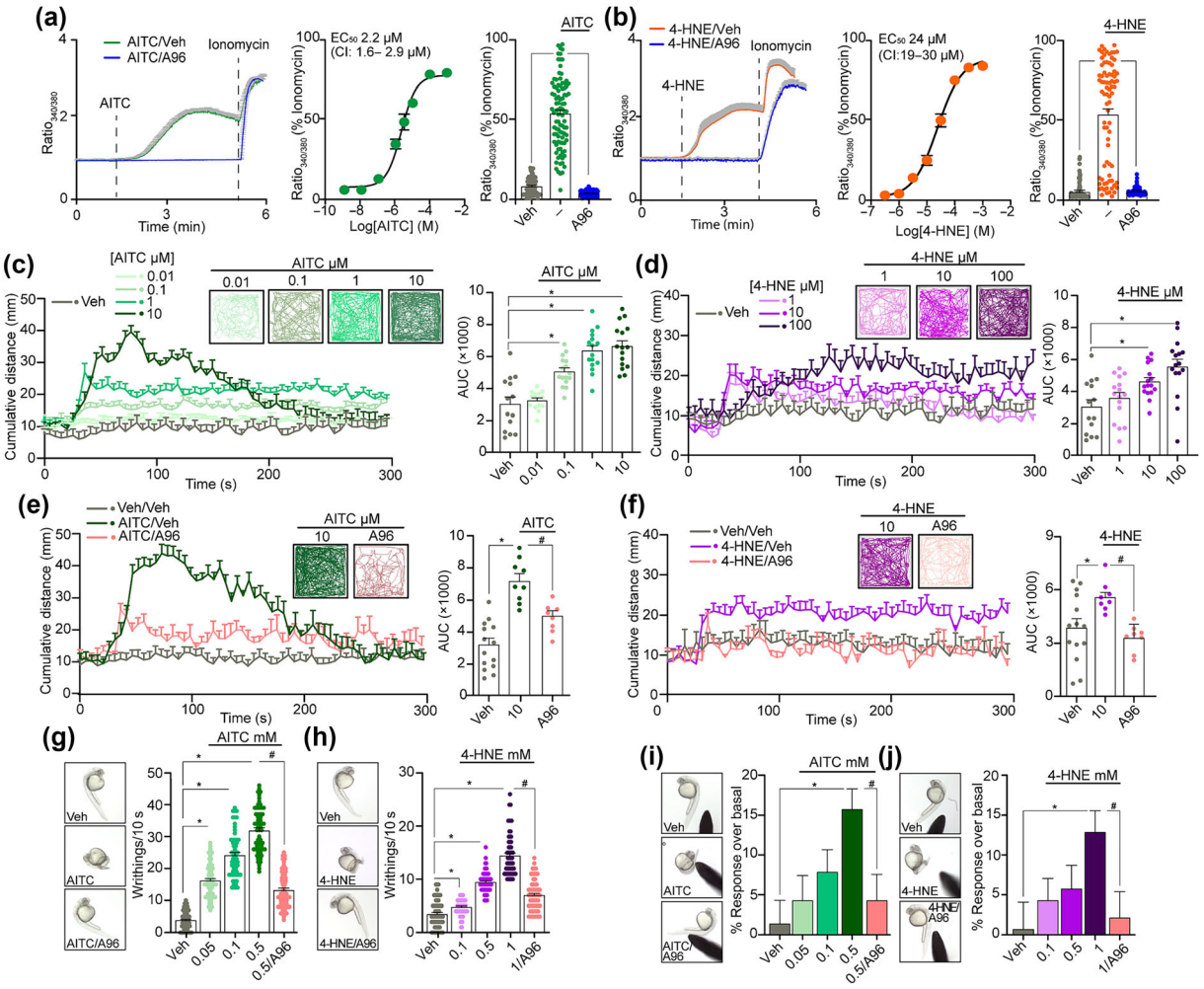

FIGURE 1 AITC and 4-HNE promote nociceptive-like behaviour in zebrafish larvae via TRPA1. (a,b) Typical traces, concentration–response curve and cumulative data of calcium responses in zTRPA1b-HEK293T cells stimulated with AITC, 4-HNE or vehicle (Veh) and in the presence of A-967079 (A96, 30 μM) (cell numbers: AITC: 1 nM n = 96, 10 nM n = 75, 100 nM n = 112, 1 μM n = 70, 3 μM n = 111, 10 μM n = 94, 100 μM n = 80, 1 mM n = 84, A96 = 85, Veh = 44; n = 3 independent experiments) (cell numbers: 4-HNE: 300 nM n = 56, 1 μM n = 52, 3 μM n = 90, 10 μM n = 77, 30 μM n = 80, 100 μM n = 98, 300 μM n = 92, 1 mM n = 64, A96 = 88, Veh = 77). (c–f) Typical traces and cumulative data of the locomotor activity of 5 days post fertilization (dpf) zebrafish larvae exposed to AITC (0.01–0.1–1–10 μM), 4-HNE (1–10–100 μM) or Veh and in the presence of A96 (10 μM) (n = 8–16 larvae per group). (g,h) Typical images and dose-dependent writhing behaviour in 24–27 post fertilization (hpf) zebrafish larvae exposed to AITC (50–100–500 μM), 4-HNE (100–500 μM, 1 mM) or Veh and in the presence of A96 (30 μM) (n = 60 larvae per group). (i,j) Typical images and dose-dependent light touch response in 24–27 hpf zebrafish larvae exposed to AITC (50–100–500 μM), 4-HNE (100–500 μM, 1 mM) or Veh and in the presence of A96 (30 μM) (n = 60 larvae per group). Mean ± SEM. $^{*}P < 0.05$; $^{\#}P < 0.05$, one-way ANOVA and Bonferroni post hoc test.

stimulation of zTRPA1b-transiently transfected HEK293T cells with H_2O_2 induced a concentration (10 μM to 1 mM)-dependent calcium response that was prevented by A-967079 (Figure 2a). Exposure of 5 days post fertilization zebrafish larvae to H_2O_2 (100–1000 μM) elicited increased locomotor activity that was attenuated by pretreatment with A-967079 (Figure 2b,c). Zebrafish larvae (24–27 post fertilization) stimulated with H_2O_2 also showed a dose-dependent (30–100–300 μM) increase in the number of tail coils and responsiveness to light tactile stimuli, which were reduced by A-967079 (Figure 2d,e). These data confirm that zTRPA1 exhibits the mammalian features of an oxidative stress sensor that mediates both the acute nociceptive response and the sensitization to mechanical stimuli.

3.3 | Oxaliplatin sensitizes TRPA1 to oxidative stress

The platinum-based anticancer drug, oxaliplatin, was found to elicit mechanical allodynia in rodents by generating oxidative stress (Joseph et al., 2008; Kopetz et al., 2009) and by targeting TRPA1 (Nassini et al., 2011). To understand whether and how oxaliplatin induces a CIPN-like condition in zebrafish, acetylated tubulin (α-**tubulin**) was assessed by whole-mount immunofluorescence in larvae incubated with oxaliplatin from 1 to 5 days post fertilization (Khan et al., 2012; Lisse et al., 2016). Oxaliplatin induced a dose-dependent reduction in α-tubulin, indicating axon degeneration (Figure 3a) by the toxic action of oxaliplatin.

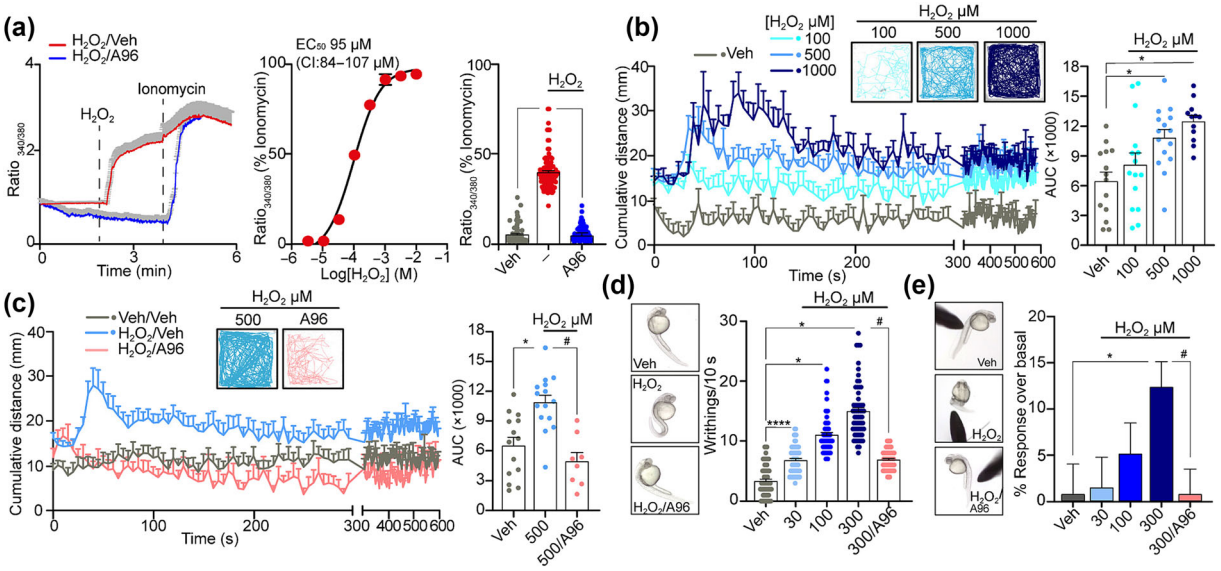

FIGURE 2 H_2O_2 induces nociceptive-like behaviour in zebrafish larvae via TRPA1. (a) Typical traces, concentration–response curve and cumulative data of calcium responses in zTRPA1b-HEK293T cells exposed to H_2O_2 or vehicle (Veh) and in the presence of A-967079 (A96, 30 µM) (cell numbers: H_2O_2: 3 µM n = 120, 10 µM n = 93, 30 µM n = 78, 100 µM n = 81, 300 µM n = 90, 1 mM n = 83, 3 mM n = 90, 10 mM n = 99, A96 = 110, Veh = 77). (b,c) Typical traces and cumulative data of the locomotor activity of 5 days post fertilization (dpf) zebrafish larvae exposed to H_2O_2 (100–500 µM, 1 mM) or Veh and in the presence of A96 (10 µM) (n = 8–15 larvae per group). (d) Typical images and dose-dependent writhing behaviour in 24–27 post fertilization (hpf) zebrafish larvae exposed to H_2O_2 (30–100–300 mM) or Veh and in the presence of A96 (30 µM) (n = 60 larvae per group). (e) Typical images and dose-dependent light touch response in 24–27 hpf zebrafish larvae exposed to H_2O_2 (30–100–300 mM) or Veh and in the presence of A96 (30 µM) (n = 60 larvae per group). Mean ± SEM. $^{*}P < 0.05$; $^{\#}P < 0.05$ one-way ANOVA and Bonferroni post hoc test.

Four days of oxaliplatin (1–10 µM) exposure to zebrafish larvae dose dependently increased locomotor activity (Figure 3b). Using transparent Casper zebrafish larvae expressing the H_2O_2 genetically encoded biosensor, Hyper7, we observed that oxaliplatin increased Hyper7 fluorescence, a response that was prevented in the presence of the antioxidant, GSH (Figure 3c). GSH also inhibited the increased locomotor activity following oxaliplatin, thus revealing the contribution of oxidative stress in this pain-like behaviour (Figure 3d). Similarly, selective TRPA1 blockade by A-967079 reduced both Hyper7 fluorescence and locomotor activity (Figure 3e,f). The combination of a dose of oxaliplatin, per se insufficient to increase the locomotor activity, and a normal subthreshold dose of H_2O_2 increased locomotor activity. This response was reduced by the TRPA1 antagonist, A-967079, and by the antioxidant, **glutathione (GSH**; Figure 3g,h). A combination of subthreshold concentrations of oxaliplatin and AITC increased the locomotory activity that was reduced in the presence of A-967079 or GSH (Figure 3i).

In vitro data also reported the ability of a subthreshold concentration of H_2O_2 to activate the zTRPA1 channel following oxaliplatin exposure. In zTRPA1b-HEK293T cells, a combination of ineffective concentrations of oxaliplatin and subthreshold H_2O_2 induced a significantly increased calcium response that was reduced in the presence of A-967079 or GSH (Figure 3j). Altogether, these data indicate that TRPA1 exerts a dual proalgesic activity in zebrafish larvae exposed to oxaliplatin: on one hand it is gated by the oxidative stress generated by oxaliplatin and on the other hand, by amplifying oxidative stress, maintaining the pain-like signal.

3.4 | Schwann cell (SC) TRPA1 amplifies oxidative stress to sustain pain-like response in mice and zebrafish chemotherapy-peripheral neuropathy (CIPN) models

Recently, we revealed the key role of SC TRPA1 in the oxidative stress generation that sustains mechanical allodynia in mouse models evoked by partial sciatic nerve ligation, alcohol polyneuropathy, cancer and the pro-migraine agent, calcitonin gene-related peptide (CGRP) (De Logu et al., 2020, 2017, 2022; De Logu, Marini, et al., 2021; Landini et al., 2023). Thus, we wondered whether SC TRPA1 contributes to CIPN in mice and zebrafish larvae. To this purpose, mice with selective and conditional deletion of TRPA1 in SC (*Plp1*$^{+}$-*Trpa1*) received a single administration of oxaliplatin (3 mg·kg^{-1}) (Nassini et al., 2011). Efficiency of TRPA1 deletion in SCs was confirmed by a reduction of TRPA1 immunoreactivity in S100+ cells in sciatic nerve (Figure S1a). As previously reported in C57BL/6J mice (Nassini et al., 2011), oxaliplatin induces a time-dependent mechanical allodynia in control mice, a response that was reduced in *Plp1*$^{+}$-*Trpa1* (Figure 4a). In addition, the increased 4-HNE levels in sciatic nerve of control mice treated with oxaliplatin were attenuated in *Plp1*$^{+}$-*Trpa1* (Figure 4b). These findings suggest that, in mice, SC

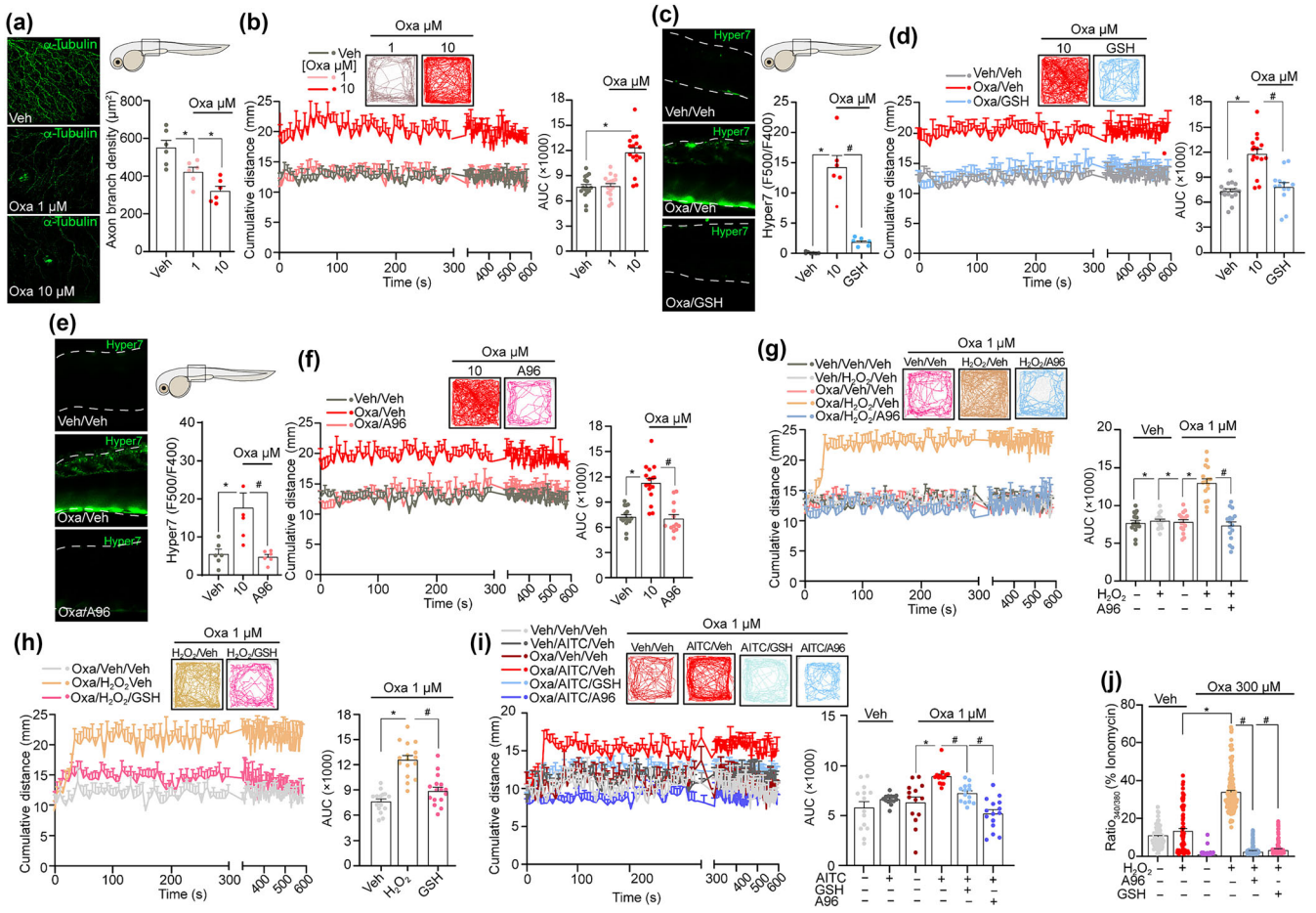

FIGURE 3 Oxaliplatin increases oxidative stress, which targets TRPA1 to induce nociceptive behaviour and calcium response. (a) Schematic representation of zebrafish larvae body section and representative images of the lateral view of 5 days post fertilization (dpf) zebrafish larvae stained with anti-acetylated tubulin (α-tubulin) and cumulative data of axon branch density following exposure to oxaliplatin (Oxa, 1–10 μM) or vehicle (Veh) (n = 6 larvae per group). (b) Typical traces and cumulative data of the locomotor activity of 5 dpf zebrafish larvae exposed to Oxa (1–10 μM). (c) Schematic representation of zebrafish larvae body section and representative images of the lateral view of 5 dpf zebrafish larvae injected with Hyper7 mRNA at one-cell stage and cumulative data of HyPer ratio (YFP500/YFP400) fluorescence following exposure to Oxa (10 μM) or Veh and in the presence of reduced glutathione (GSH, 10 μM) (n = 6 larvae per group). (d) Typical traces and cumulative data of the locomotor activity of 5 dpf zebrafish larvae exposed to Oxa (10 μM) or Veh and in the presence of GSH (10 μM) (n = 13–16 larvae per group). (e) Schematic representation of zebrafish larvae body section and representative images of the lateral view of 5 dpf zebrafish larvae injected with Hyper7 mRNA at one-cell stage and cumulative data of HyPer ratio (YFP500/YFP400) fluorescence following exposure to Oxa (10 μM) or Veh and in the presence of A-967079 (A96, 1 μM) (n = 6 larvae per group). (f) Typical traces and cumulative data of locomotor activity of 5 dpf zebrafish larvae exposed to Oxa (10 μM) or Veh and in the presence of A96 (10 μM) (n = 16 larvae per group). (g–i) Typical traces and cumulative data of the locomotor activity of 5 dpf exposed to a subthreshold dose of H_2O_2 (100 μM) and AITC (0.01 μM) or Veh following incubation with a subthreshold dose of Oxa (1 μM) or Veh and in the presence of A96 (10 μM) or GSH (10 μM) (n = 16 larvae per group). (j) Cumulative data of the calcium response evoked by subthreshold concentration of H_2O_2 (30 μM) in zTRPA1b-HEK293T cells pre-incubated with Oxa (300 μM) or Veh in the absence or presence of A96 (30 μM) or GSH (30 μM) (cell numbers: Veh-Veh n = 83, Veh-H_2O_2 n = 78, Veh-Oxa n = 111, Oxa-H_2O_2 n = 129, Oxa-H_2O_2-A96 n = 156, Oxa-H_2O_2-GSH n = 148; n = 3 independent experiments). Mean ± SEM. $^*P < 0.05$, $^\#P < 0.05$, one-way ANOVA and Bonferroni post hoc test.

TRPA1 amplifies the oxidative burden that sensitizes sciatic nerve fibres after exposure to oxaliplatin. In line with previous reports in various mouse pain models (De Logu et al., 2019, 2020, 2022; De Logu, Marini, et al., 2021; Landini et al., 2022), selective deletion of TRPA1 in mouse primary sensory neurons (*Adv*$^+$-*Trpa1*) (Figure S1b) attenuated mechanical allodynia elicited by oxaliplatin (Figure 4c), thus confirming the key role of neuronal TRPA1 as the final target of the SC/TRPA1/oxidative stress pathway in pain signalling.

Next, we explored whether results obtained in mice could be reproduced in zebrafish. First, we reported that zebrafish larvae (5 days post fertilization) peripheral nerves positive for α-tubulin showed SOX10 staining, as expected for SCs (Kamenev et al., 2021; McGraw et al., 2008; Xie et al., 2019) (Figure 4d). To confirm the expression of TRPA1 channel in larvae SCs, we used combined immunofluorescence and RNAscope. SOX10 positive nuclei were superimposed with the RNAscope probe for *trpa1b* (Figure 4e). Furthermore,

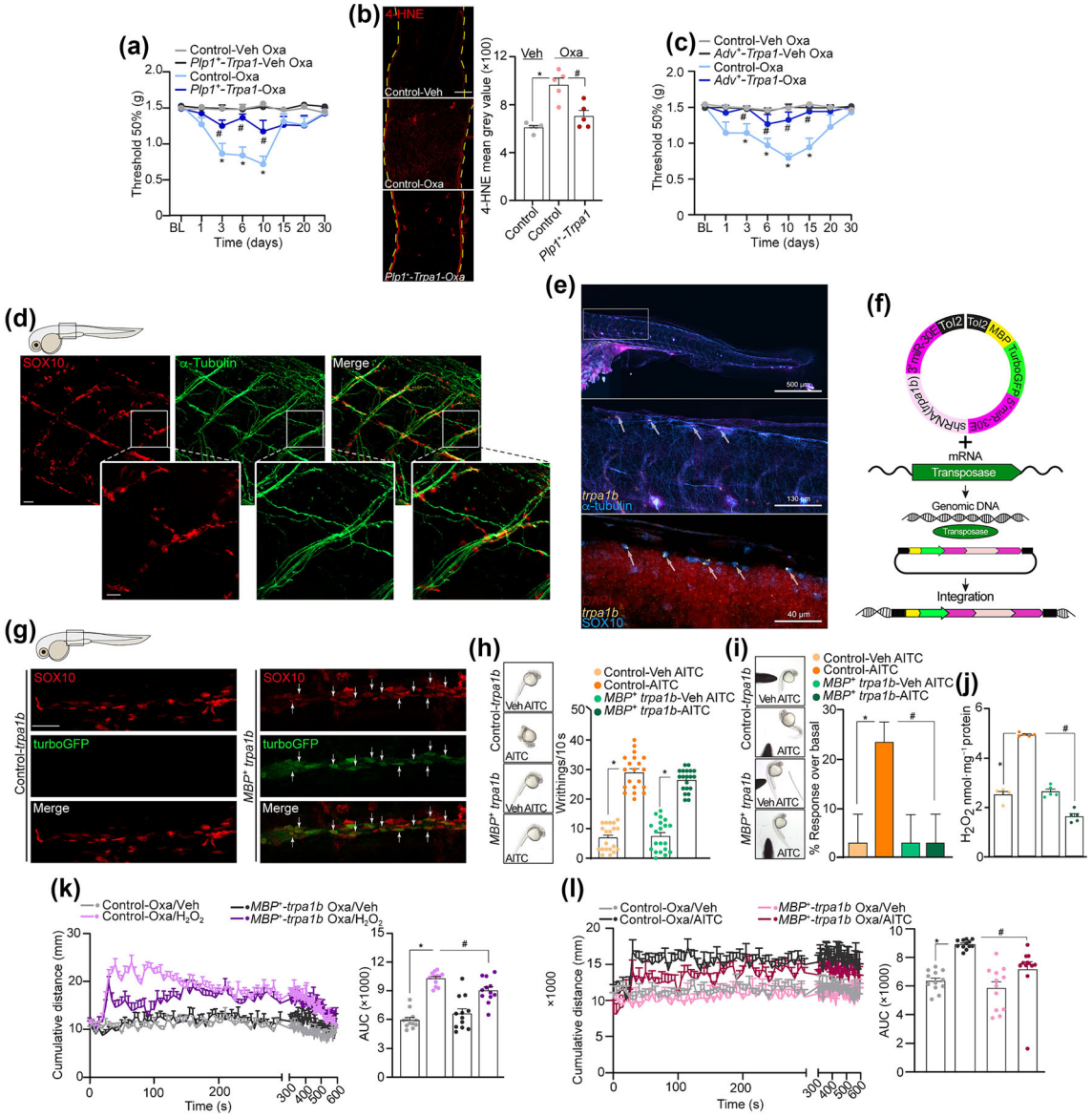

FIGURE 4 Schwann cell TRPA1 modulates painful behaviours in oxaliplatin-induced CIPN. (a) Time-dependent mechanical allodynia induced by oxaliplatin (Oxa, 3 mg·kg^{-1}, i.p.) or vehicle (Veh) in *Plp1*$^{+}$*-Trpa1* and control mice (n = 8 animals per group). (b) Representative images and cumulative data of 4-HNE immunostaining in mouse sciatic nerve tissue in *Plp1*$^{+}$*-Trpa1* and control mice after Oxa (3 mg·kg^{-1}, i.p.) or Veh (scale bar: 50 μm) (n = 5 animals per group, yellow dashes represent the edge of sciatic nerve). (c) Time-dependent mechanical allodynia induced by oxaliplatin (Oxa, 3 mg·kg^{-1}, i.p.) or Veh in *Adv*$^{+}$*-Trpa1* and control mice (n = 8 animals per group). (d) Schematic representation of zebrafish larvae body section and representative images of the lateral view of 5 days post fertilization (dpf) zebrafish larvae stained with anti-acetylated tubulin (α-tubulin, axons marker) and SOX10 (Schwann cells marker) (scale bar: 20 μm). (e) Representative images of the lateral view of RNAscope images of *TRPA1b* mRNA, SOX10 and α-tubulin in 5 dpf zebrafish larvae. (f) Schematic representation of pTol2-MBP-TurboGFP-dre-trpa1_b[shRNA] plasmid. (g) Schematic representation of zebrafish larvae body section and representative images of SOX10 immunostaining and turbo GFP protein in 5 dpf *MBP*$^{-}$*-trpa1b* zebrafish larvae (scale bar: 10 μm). (h,i) Writhing behaviour and light touch response in 24–27 post fertilization (hpf) *MBP*$^{+}$*-trpa1b* or control zebrafish larvae exposed to AITC (500 μM) or Veh (n = 20 larvae per group). (j) H_2O_2 levels in 5 dpf *MBP*$^{+}$*-trpa1b* or control zebrafish larvae homogenates exposed to AITC (10 μM) or Veh (n = 5 larvae per group). (k,l) Time-dependent and cumulative data of the locomotor activity of 5 dpf *MBP*$^{+}$*-trpa1b* or control zebrafish larvae exposed to a subthreshold dose of H_2O_2 (100 μM) and AITC (0.01 μM) or Veh following incubation with a subthreshold dose of Oxa (1 μM) (n = 12 larvae per group). Mean ± SEM. $^{*}P < 0.05$ (vs. Control-Veh-Oxa in a); $^{\#}P < 0.05$ (vs. Control-Oxa in a) one-way and two-way ANOVA and Bonferroni post hoc test.

to identify the role of SC TRPA1 in mediating pain behaviour in zebrafish larvae, one-cell-stage zebrafish embryos were injected with an shRNA-(*trpa1b*) expression plasmid under the control of SC selective myelin basic protein (MBP) promoter (*MBP*$^{+}$*-trpa1b* zebrafish larvae) (Figure 4f) (Gow et al., 1992). Selective silencing of *trpa1b* in zebrafish SC was confirmed by co-expression of the gene reporter TurboGFP and the SC marker SOX10 (Figure 4g) and the reduction of *trpa1b* RNAscope probe fluorescence in SOX10 positive cells (Figure S1c).

Trpa1b selective silencing in MBP cells in *MBP*$^{+}$*-trpa1b* zebrafish larvae did not affect the number of tail coils (Figure 4h) but conversely reduced the light touch responses following AITC stimulation in 24–27 post fertilization zebrafish larvae (Figure 4i). In addition, the increased H_2O_2 levels observed in control *MBP*$^{-}$*-trpa1b* zebrafish larvae after AITC stimulation were reduced in *MBP*$^{+}$*-trpa1b* zebrafish larvae at the same developmental stage (Figure 4j), thus confirming a role of SC TRPA1 in amplifying oxidative stress. Moreover, the increased locomotor activity in zebrafish larvae incubated with a subthreshold dose of oxaliplatin and stimulated with a subthreshold dose of either H_2O_2 or AITC was reduced in *MBP*$^{+}$*-trpa1b* zebrafish larvae (Figure 4k,l). These data confirm a role of SC TRPA1 as a pain sensor in CIPN in mice and in zebrafish larvae and its role as ROS enhancer to sustain pain-like behaviours.

4 | DISCUSSION

In this study, we found that the exposure of zebrafish larvae to oxaliplatin increases mechanical sensitivity, a response that recapitulates the primary sensory alteration (mechanical allodynia) produced in mice by the anticancer drug (Nassini et al., 2011). TRPA1 has been identified as a major oxidant sensor and signal integrator for excitation in response to oxidative stress increase (Bessac et al., 2008; Takahashi & Mori, 2011). The role of TRPA1 as a sensor and amplifier of oxidative stress in mammals has also been described in zebrafish. Here, we first tested the role of zTRPA1 as an oxidant sensor. Previous data reported that direct TRPA1 stimulation with selective channel agonists, such as AITC and 4-HNE, induced a behavioural response in zebrafish larvae and embryos (Ko et al., 2019; Prober et al., 2008; Stevens et al., 2018). Cells expressing the two zTRPA1 paralogs were activated by several chemical irritants *in vitro* (Prober et al., 2008). Here, in addition to AITC and 4-HNE, we report that H_2O_2 induces a calcium response in cells transfected with zTRPA1. Furthermore, exposure of zebrafish larvae to H_2O_2 increases a series of nociceptive responses, including locomotor activity, number of tail coils and ensuing sensitization to light touch, all dependent on TRPA1 activation, thus confirming that zTRPA1 possesses the mammalian features of an oxidative stress sensor.

Chemotherapeutic agents, including oxaliplatin/**cisplatin**, increase ROS and their by-products in plasma, cells and tissues of treated animals or patients, and ROS scavengers or antioxidants show some degree of protection against chemotherapy-induced peripheral neuropathy (CIPN) in humans or their rodent counterparts (Jaggi & Singh, 2012). Here, we confirm that an antioxidant or TRPA1 antagonist reduces the pain-like behavioural response associated to a CIPN model induced by oxaliplatin in zebrafish, as previously found in rodent models of CIPN (Nassini et al., 2011). Taken together, these findings indicate that TRPA1, via its activation by oxidative stress by-products, is necessary and sufficient to produce a neuropathy paradigm in a zebrafish model of CIPN.

Several preclinical studies and clinical investigations have found that neurons play a key role in CIPN; altered activity of voltage gated ion channel (Adelsberger et al., 2000; Boyette-Davis et al., 2015; Zajaczkowska et al., 2019), increased neurotransmission (Boyette-Davis et al., 2015), sensibilization of TRP channels (Boyette-Davis et al., 2015; Chukyo et al., 2018; Yamamoto et al., 2015) and increased neuroinflammation (Fumagalli et al., 2020) are reported as some of the molecular mechanisms that define a neuron dysfunction as the cause of CIPN. While neurons play a central and exclusive role in receiving and transmitting pain signals, non-neuronal cells, including glial cells (Vallejo et al., 2010), astrocytes (Gao et al., 2009; Robinson et al., 2014) and satellite glial cells (Warwick & Hanani, 2013), are receiving evermore attention for their function as a promoter of a proalgesic phenotype in CIPN.

Recently, we reported that Schwann cells (SCs), a primary glial cell type that protects and nurtures all peripheral nerve fibres and speeds up transmission velocity via the myelin sheet, are key contributors to sustain pain signals in mouse models of neuropathic (De Logu et al., 2017), cancer (De Logu, Marini, et al., 2021; Landini et al., 2022) and migraine (De Logu et al., 2022) pain. ROS produced under neuroinflammatory conditions target SC TRPA1 that, in a calcium-dependent manner, activates **NADPH oxidase 1 (NOX1)** to promote the feed-forward mechanism that sustains the release of ROS and the ensuing mechanical hyperalgesia (De Logu et al., 2020, 2017). Accumulating evidence implicates immune-mediated processes in CIPN, highlighted by immune cell infiltration into peripheral nerve tissue and phenotypic changes of peripheral glial cells (Kiguchi et al., 2008; Liu et al., 2016; Peters et al., 2007). A SC contribution in CIPN has been reported. SC treatment with taxanes induces cytotoxicity and downregulation of the myelin basic protein (MBP) expression (Imai et al., 2017). Intraperitoneal (i.p.) injection of paclitaxel in mice induces the upregulation of the macrophage recruiter molecule **galectin-3** in cultured SCs and peripheral nerves (Koyanagi et al., 2021). SC gene expression analysis indicates endoplasmic reticulum damage followed by the downregulation of myelin-related genes in patients after a high dose of bortezomib (Filosto et al., 2007; Shin et al., 2010).

Here, we report that selective silencing of *Trpa1* in mouse SCs reduces the accumulation of the oxidative stress by-product, 4-HNE, in the sciatic nerve and mechanical allodynia induced by oxaliplatin administration. In addition, the selective silencing of *Trpa1* in mouse primary sensory neurons also reduces mechanical allodynia. Taken together, these findings confirm the critical role of SCs in sustaining mechanical allodynia by amplifying oxidative stress generation that, finally, targets the neuronal TRPA1. The pathway revealed here for the CIPN model of peripheral polyneuropathy has been previously reported in rodent models of neuropathic (De Logu et al., 2020, 2017) or cancer (De Logu, Marini, et al., 2021; Landini et al., 2022) pain. Here, we extended this hypothesis to zebrafish, implicating SC TRPA1 as a conserved proalgesic pathway across the animal kingdom. RNAScope assay revealed that the SOX10+ (SC marker) cells in zebrafish express the *Trpa1* mRNA, as previously reported in C57BL/6J mice (Al-Omari et al., 2022). Expression of an H_2O_2 genetically encoded biosensor showed a TRPA1-dependent increase in H_2O_2 in larvae exposed to oxaliplatin.

A shRNA for zebrafish *Trpa1* under the selective SC promoter (MBP) selectively silenced *Trpa1* expression in SCs. *Trpa1* silencing in zebrafish SCs did not affect the early tail coil response evoked by the TRPA1 selective agonist, AITC. This response occurs immediately after exposure to the stimulus and is most likely dependent on a direct activation of neuronal TRPA1. These results are consistent with findings obtained previously in mice showing that the early, spontaneous nociceptive response to AITC was not reduced by SC TRPA1 silencing (De Logu et al., 2017). However, selective TRPA1 antagonism or genetic silencing in SCs reduced the light touch response, a phenomenon that may recall the mechanical allodynia produced in mice by a variety of stimuli (De Logu et al., 2017). Moreover, *Trpa1* silencing in zebrafish SCs reduced H_2O_2 increase and locomotor activity, evoked by subthreshold concentrations of AITC and oxaliplatin. Overall, these methods confirmed in zebrafish the data obtained in mice (De Logu et al., 2017) that SC TRPA1 amplifies the oxidative stress signal. One limitation of the study is the relative efficiency of target gene deletion (in mice) and gene silencing (in zebrafish larvae) that may explain the incomplete reduction of mechanical allodynia in mice and locomotor activity in zebrafish larvae associated with these genetic interventions. Our findings report that oxaliplatin, an important and widely used chemotherapeutic agent, causes changes at both behavioural (increased locomotor activity) and cellular levels (reduction in the density of sensory innervation) in zebrafish larvae, implicating that the functions of SC TRPA1 and oxidative stress are remarkably similar, if not identical, to those of mice in the oxaliplatin CIPN model.

5 | CONCLUSION

Although the practical advantages in the study of rodent models are emphasized for their similarities in genetic and pathophysiological features with humans, the easy maintenance and rapid experimental manipulations of zebrafish provide an *in vivo* model that allows a facilitated approach for the study of SCs, TRPA1 and the oxidative stress role in mediating painful behavioural responses of chemotherapeutics and possible other pain stimuli and conditions.

AUTHOR CONTRIBUTIONS

E. Bellantoni, C. Gabellini, E. L. Crapanzano and L. Roschi performed in vivo experiments and helped to draft the manuscript; M. Marini and M. Chieca performed in vitro experiments and helped to draft the manuscript; D. Souza Monteiro de Araujo and D. Nosi performed RNAscope and immunofluorescence and helped to draft the manuscript; and P. Geppetti, R. Nassini and F. De Logu conceived, designed, reviewed and edited the paper. All authors reviewed and approved the manuscript.

ACKNOWLEDGEMENTS

This work was supported by Fondazione Cassa di Risparmio di Firenze–Human Brain Optical Mapping Project (P.G.); Fondazione Telethon (Grant GMR22T1070); European Union—Next Generation EU, National Recovery and Resilience Plan, Mission 4 Component 2—Investment 1.4—National Center for Gene Therapy and Drugs based on RNA Technology (CUP B13C22001010001) (R.N.); and Mission 4 Component 2—Investment 1.3—Mnesys A multiscale integrated approach to the study of the nervous system in health and disease (CUP B83C22004910002) (P.G. and F.D.L.). Views and opinions expressed are those of the author (s) only and do not necessarily reflect those of the European Union or the European Commission. Neither the European Union nor the European Commission can be held responsible for these opinions. Open access publishing facilitated by Universita degli Studi di Firenze, as part of the Wiley - CRUI-CARE agreement.

CONFLICT OF INTEREST STATEMENT

R.N., F.D.L. and P.G. are founding scientists of FloNext Srl. Other authors declare no competing interest.

DATA AVAILABILITY STATEMENT

Materials and data generated from this study are available upon request from the corresponding author.

DECLARATION OF TRANSPARENCY AND SCIENTIFIC RIGOUR

This Declaration acknowledges that this paper adheres to the principles for transparent reporting and scientific rigour of preclinical research as stated in the *BJP* guidelines for Design and Analysis, Immunoblotting and Immunochemistry and Animal Experimentation, and as recommended by funding agencies, publishers and other organizations engaged with supporting research.

ORCID

Matilde Marini https://orcid.org/0000-0002-2199-2905
Chiara Gabellini https://orcid.org/0000-0002-5544-1570
Daniel Souza Monteiro de Araujo https://orcid.org/0000-0003-1115-725X
Lorenzo Landini https://orcid.org/0000-0002-3933-2497
Gaetano De Siena https://orcid.org/0000-0003-3600-9130
Pasquale Pensieri https://orcid.org/0000-0003-4914-3144
Pierangelo Geppetti https://orcid.org/0000-0003-3797-8371
Romina Nassini https://orcid.org/0000-0002-9223-8395
Francesco De Logu https://orcid.org/0000-0001-8360-6929

REFERENCES

Adelsberger, H., Quasthoff, S., Grosskreutz, J., Lepier, A., Eckel, F., & Lersch, C. (2000). The chemotherapeutic oxaliplatin alters voltage-gated Na^+ channel kinetics on rat sensory neurons. *European Journal of Pharmacology*, *406*, 25–32. https://doi.org/10.1016/S0014-2999(00)00667-1

Alexander, S. P. H., Christopoulos, A., Davenport, A. P., Kelly, E., Mathie, A. A., Peters, J. A., Veale, E. L., Armstrong, J. F., Faccenda, E., Harding, S. D., Davies, J. A., Abbracchio, M. P., Abraham, G., Agoulnik, A., Alexander, W., Al-Hosaini, K., Bäck, M., Baker, J. G., Barnes, N. M., … Ye, R. D. (2023a). The Concise Guide to PHARMACOLOGY 2023/24: G protein-coupled receptors. *British Journal of Pharmacology*, *180*, S23–S144. https://doi.org/10.1111/bph.16177

Alexander, S. P. H., Mathie, A. A., Peters, J. A., Veale, E. L., Striessnig, J., Kelly, E., Armstrong, J. F., Faccenda, E., Harding, S. D., Davies, J. A.,

Aldrich, R. W., Attali, B., Baggetta, A. M., Becirovic, E., Biel, M., Bill, R. M., Caceres, A. I., Catterall, W. A., Conner, A. C., & Zhu, M. (2023b). The Concise guide to PHARMACOLOGY 2023/24: Ion channels. *British Journal of Pharmacology*, *180*(Suppl 2), S145–s222. https://doi.org/10.1111/bph.16178

Alexander, S. P. H., Roberts, R. E., Broughton, B. R. S., Sobey, C. G., George, C. H., Stanford, S. C., Cirino, G., Docherty, J. R., Giembycz, M. A., Hoyer, D., Insel, P. A., Izzo, A. A., Ji, Y., MacEwan, D. J., Mangum, J., Wonnacott, S., & Ahluwalia, A. (2018). Goals and practicalities of immunoblotting and immunohistochemistry: A guide for submission to the *British Journal of Pharmacology*. *British Journal of Pharmacology*, *175*, 407–411. https://doi.org/10.1111/bph.14112

Al-Omari, A., Kecskés, M., Gaszner, B., Biró-Sütő, T., Fazekas, B., Berta, G., Kuzma, M., Pintér, E., & Kormos, V. (2022). Functionally active TRPA1 ion channel is downregulated in peptidergic neurons of the Edinger-Westphal nucleus upon acute alcohol exposure. *Frontiers in Cell and Development Biology*, *10*, 1046559.

Andersson, D. A., Gentry, C., Moss, S., & Bevan, S. (2008). Transient receptor potential A1 is a sensory receptor for multiple products of oxidative stress. *The Journal of Neuroscience*, *28*, 2485–2494. https://doi.org/10.1523/JNEUROSCI.5369-07.2008

Banach, M., Juranek, J. K., & Zygulska, A. L. (2017). Chemotherapy-induced neuropathies—A growing problem for patients and health care providers. *Brain and Behavior: A Cognitive Neuroscience Perspective*, *7*, e00558. https://doi.org/10.1002/brb3.558

Bessac, B. F., Sivula, M., von Hehn, C. A., Escalera, J., Cohn, L., & Jordt, S. E. (2008). TRPA1 is a major oxidant sensor in murine airway sensory neurons. *The Journal of Clinical Investigation*, *118*, 1899–1910. https://doi.org/10.1172/JCI34192

Boyette-Davis, J. A., Walters, E. T., & Dougherty, P. M. (2015). Mechanisms involved in the development of chemotherapy-induced neuropathy. *Pain Management*, *5*, 285–296. https://doi.org/10.2217/pmt.15.19

Chaplan, S. R., Bach, F. W., Pogrel, J. W., Chung, J. M., & Yaksh, T. L. (1994). Quantitative assessment of tactile allodynia in the rat paw. *Journal of Neuroscience Methods*, *53*, 55–63. https://doi.org/10.1016/0165-0270(94)90144-9

Chukyo, A., Chiba, T., Kambe, T., Yamamoto, K., Kawakami, K., Taguchi, K., & Abe, K. (2018). Oxaliplatin-induced changes in expression of transient receptor potential channels in the dorsal root ganglion as a neuropathic mechanism for cold hypersensitivity. *Neuropeptides*, *67*, 95–101. https://doi.org/10.1016/j.npep.2017.12.002

Cirrincione, A. M., & Rieger, S. (2020). Analyzing chemotherapy-induced peripheral neuropathy in vivo using non-mammalian animal models. *Experimental Neurology*, *323*, 113090. https://doi.org/10.1016/j.expneurol.2019.113090

Curtis, M. J., Alexander, S. P. H., Cirino, G., George, C. H., Kendall, D. A., Insel, P. A., Izzo, A. A., Ji, Y., Panettieri, R. A., Patel, H. H., Sobey, C. G., Stanford, S. C., Stanley, P., Stefanska, B., Stephens, G. J., Teixeira, M. M., Vergnolle, N., & Ahluwalia, A. (2022). Planning experiments: Updated guidance on experimental design and analysis and their reporting III. *British Journal of Pharmacology*., *179*, 3907–3913. https://doi.org/10.1111/bph.15868

Curtright, A., Rosser, M., Goh, S., Keown, B., Wagner, E., Sharifi, J., Raible, D. W., & Dhaka, A. (2015). Modeling nociception in zebrafish: A way forward for unbiased analgesic discovery. *PLoS ONE*, *10*, e0116766. https://doi.org/10.1371/journal.pone.0116766

De Logu, F., De Prá, S. D., de David Antoniazzi, C. T., Kudsi, S. Q., Ferro, P. R., Landini, L., Rigo, F. K., de Bem Silveira, G., Silveira, P. C. L., Oliveira, S. M., Marini, M., Mattei, G., Ferreira, J., Geppetti, P., Nassini, R., & Trevisan, G. (2020). Macrophages and Schwann cell TRPA1 mediate chronic allodynia in a mouse model of complex regional pain syndrome type I. *Brain, Behavior, and Immunity*, *88*, 535–546. https://doi.org/10.1016/j.bbi.2020.04.037

De Logu, F., De Siena, G., Landini, L., Marini, M., Souza Monteiro de Araujo, D., Albanese, V., Preti, D., Romitelli, A., Chieca, M., Titiz, M., & Iannone, L. F. (2023). Non-neuronal TRPA1 encodes mechanical allodynia associated with neurogenic inflammation and partial nerve injury in rats. *British Journal of Pharmacology*, *180*(9), 1232–1246. https://doi.org/10.1111/bph.16005

De Logu, F., Li Puma, S., Landini, L., Portelli, F., Innocenti, A., de Araujo, D. S. M., Janal, M. N., Patacchini, R., Bunnett, N. W., Geppetti, P., & Nassini, R. (2019). Schwann cells expressing nociceptive channel TRPA1 orchestrate ethanol-evoked neuropathic pain in mice. *The Journal of Clinical Investigation*, *129*, 5424–5441. https://doi.org/10.1172/JCI128022

De Logu, F., Marini, M., Landini, L., Souza Monteiro de Araujo, D., Bartalucci, N., Trevisan, G., Bruno, G., Marangoni, M., Schmidt, B. L., Bunnett, N. W., & Geppetti, P. (2021). Peripheral nerve resident macrophages and Schwann cells mediate cancer-induced pain. *Cancer Research*, *81*, 3387–3401. https://doi.org/10.1158/0008-5472.CAN-20-3326

De Logu, F., Nassini, R., Hegron, A., Landini, L., Jensen, D. D., Latorre, R., Ding, J., Marini, M., Souza Monteiro de Araujo, D., Ramírez-Garcia, P., Whittaker, M., Retamal, J., Titiz, M., Innocenti, A., Davis, T. P., Veldhuis, N., Schmidt, B. L., Bunnett, N. W., & Geppetti, P. (2022). Schwann cell endosome CGRP signals elicit periorbital mechanical allodynia in mice. *Nature Communications*, *13*, 646. https://doi.org/10.1038/s41467-022-28204-z

De Logu, F., Nassini, R., Materazzi, S., Carvalho Gonçalves, M., Nosi, D., Rossi Degl'Innocenti, D., Marone, I. M., Ferreira, J., Li Puma, S., Benemei, S., Trevisan, G., Souza Monteiro de Araújo, D., Patacchini, R., Bunnett, N. W., & Geppetti, P. (2017). Schwann cell TRPA1 mediates neuroinflammation that sustains macrophage-dependent neuropathic pain in mice. *Nature Communications*, *8*, 1887. https://doi.org/10.1038/s41467-017-01739-2

De Logu, F., Souza Monteiro de Araujo, D., Ugolini, F., Iannone, L. F., Vannucchi, M., Portelli, F., Landini, L., Titiz, M., De Giorgi, V., Geppetti, P., & Massi, D. (2021). The TRPA1 channel amplifies the oxidative stress signal in melanoma. *Cells*, *10*(11), 3131. https://doi.org/10.3390/cells10113131

Fallon, M. T. (2013). Neuropathic pain in cancer. *British Journal of Anaesthesia*, *111*, 105–111. https://doi.org/10.1093/bja/aet208

Faucherre, A., Nargeot, J., Mangoni, M. E., & Jopling, C. (2013). *piezo2b* regulates vertebrate light touch response. *The Journal of Neuroscience*, *33*, 17089–17094. https://doi.org/10.1523/JNEUROSCI.0522-13.2013

Faul, F., Erdfelder, E., Lang, A. G., & Buchner, A. (2007). G*Power 3: A flexible statistical power analysis program for the social, behavioral, and biomedical sciences. *Behavior Research Methods*, *39*, 175–191. https://doi.org/10.3758/BF03193146

Filosto, M., Rossi, G., Pelizzari, A. M., Buzio, S., Tentorio, M., Broglio, L., Mancuso, M., Rinaldi, M., Scarpelli, M., & Padovani, A. (2007). A high-dose bortezomib neuropathy with sensory ataxia and myelin involvement. *Journal of the Neurological Sciences*, *263*, 40–43. https://doi.org/10.1016/j.jns.2007.05.023

Fumagalli, G., Monza, L., Cavaletti, G., Rigolio, R., & Meregalli, C. (2020). Neuroinflammatory process involved in different preclinical models of chemotherapy-induced peripheral neuropathy. *Frontiers in Immunology*, *11*, 626687.

Gao, Y. J., Zhang, L., Samad, O. A., Suter, M. R., Yasuhiko, K., Xu, Z. Z., Park, J. Y., Lind, A. L., Ma, Q., & Ji, R. R. (2009). JNK-induced MCP-1 production in spinal cord astrocytes contributes to central sensitization and neuropathic pain. *The Journal of Neuroscience*, *29*, 4096–4108. https://doi.org/10.1523/JNEUROSCI.3623-08.2009

Goldsmith, J. R., & Jobin, C. (2012). Think small: Zebrafish as a model system of human pathology. *Journal of Biomedicine & Biotechnology*, *2012*, 817341.

Gow, A., Friedrich, V. L. Jr., & Lazzarini, R. A. (1992). Myelin basic protein gene contains separate enhancers for oligodendrocyte and Schwann cell expression. *The Journal of Cell Biology*, *119*, 605–616. https://doi.org/10.1083/jcb.119.3.605

Imai, S., Koyanagi, M., Azimi, Z., Nakazato, Y., Matsumoto, M., Ogihara, T., Yonezawa, A., Omura, T., Nakagawa, S., Wakatsuki, S., Araki, T., Kaneko, S., Nakagawa, T., & Matsubara, K. (2017). Taxanes and platinum derivatives impair Schwann cells via distinct mechanisms. *Scientific Reports*, *7*, 5947. https://doi.org/10.1038/s41598-017-05784-1

Jaggi, A. S., & Singh, N. (2012). Mechanisms in cancer-chemotherapeutic drugs-induced peripheral neuropathy. *Toxicology*, *291*, 1–9. https://doi.org/10.1016/j.tox.2011.10.019

Jordt, S. E., Bautista, D. M., Chuang, H. H., McKemy, D. D., Zygmunt, P. M., Högestätt, E. D., Meng, I. D., & Julius, D. (2004). Mustard oils and cannabinoids excite sensory nerve fibres through the TRP channel ANKTM1. *Nature*, *427*, 260–265. https://doi.org/10.1038/nature02282

Joseph, E. K., Chen, X., Bogen, O., & Levine, J. D. (2008). Oxaliplatin acts on IB4-positive nociceptors to induce an oxidative stress-dependent acute painful peripheral neuropathy. *The Journal of Pain*, *9*, 463–472. https://doi.org/10.1016/j.jpain.2008.01.335

Kamenev, D., Sunadome, K., Shirokov, M., Chagin, A. S., Singh, A., Irion, U., Adameyko, I., Fried, K., & Dyachuk, V. (2021). Schwann cell precursors generate sympathoadrenal system during zebrafish development. *Journal of Neuroscience Research*, *99*, 2540–2557. https://doi.org/10.1002/jnr.24909

Khan, T. M., Benaich, N., Malone, C. F., Bernardos, R. L., Russell, A. R., Downes, G. B., Barresi, M. J., & Hutson, L. D. (2012). Vincristine and bortezomib cause axon outgrowth and behavioral defects in larval zebrafish. *Journal of the Peripheral Nervous System*, *17*, 76–89. https://doi.org/10.1111/j.1529-8027.2012.00371.x

Kiguchi, N., Maeda, T., Kobayashi, Y., Kondo, T., Ozaki, M., & Kishioka, S. (2008). The critical role of invading peripheral macrophage-derived interleukin-6 in vincristine-induced mechanical allodynia in mice. *European Journal of Pharmacology*, *592*, 87–92. https://doi.org/10.1016/j.ejphar.2008.07.008

Kimmel, C. B., Ballard, W. W., Kimmel, S. R., Ullmann, B., & Schilling, T. F. (1995). Stages of embryonic development of the zebrafish. *Developmental Dynamics*, *203*, 253–310. https://doi.org/10.1002/aja.1002030302

Ko, M. J., Ganzen, L. C., Coskun, E., Mukadam, A. A., Leung, Y. F., & van Rijn, R. M. (2019). A critical evaluation of TRPA1-mediated locomotor behavior in zebrafish as a screening tool for novel anti-nociceptive drug discovery. *Scientific Reports*, *9*, 2430. https://doi.org/10.1038/s41598-019-38852-9

Kopetz, S., Lesslie, D. P., Dallas, N. A., Park, S. I., Johnson, M., Parikh, N. U., Kim, M. P., Abbruzzese, J. L., Ellis, L. M., Chandra, J., & Gallick, G. E. (2009). Synergistic activity of the SRC family kinase inhibitor dasatinib and oxaliplatin in colon carcinoma cells is mediated by oxidative stress. *Cancer Research*, *69*, 3842–3849. https://doi.org/10.1158/0008-5472.CAN-08-2246

Koudelka, S., Voas, M. G., Almeida, R. G., Baraban, M., Soetaert, J., Meyer, M. P., Talbot, W. S., & Lyons, D. A. (2016). Individual neuronal subtypes exhibit diversity in CNS myelination mediated by synaptic vesicle release. *Current Biology*, *26*, 1447–1455. https://doi.org/10.1016/j.cub.2016.03.070

Koyanagi, M., Imai, S., Matsumoto, M., Iguma, Y., Kawaguchi-Sakita, N., Kotake, T., Iwamitsu, Y., Ntogwa, M., Hiraiwa, R., Nagayasu, K., Saigo, M., Ogihara, T., Yonezawa, A., Omura, T., Nakagawa, S., Nakagawa, T., & Matsubara, K. (2021). Pronociceptive roles of Schwann cell-derived galectin-3 in taxane-induced peripheral neuropathy. *Cancer Research*, *81*, 2207–2219. https://doi.org/10.1158/0008-5472.CAN-20-2799

Landini, L., Marini, M., Souza Monteiro de Araujo, D., Romitelli, A., Montini, M., Albanese, V., Titiz, M., Innocenti, A., Bianchini, F., Geppetti, P., Nassini, R., & De Logu, F. (2023). Schwann cell insulin-like growth factor receptor type-1 mediates metastatic bone cancer pain in mice. *Brain, Behavior, and Immunity*, *110*, 348–364. https://doi.org/10.1016/j.bbi.2023.03.013

Landini, L., Souza Monteiro de Araujo, D., Titiz, M., Geppetti, P., Nassini, R., & De Logu, F. (2022). TRPA1 role in inflammatory disorders: What is known so far? *International Journal of Molecular Sciences*, *23*, 4529. https://doi.org/10.3390/ijms23094529

Lilley, E., Stanford, S. C., Kendall, D. E., Alexander, S. P. H., Cirino, G., Docherty, J. R., George, C. H., Insel, P. A., Izzo, A. A., Ji, Y., Panettieri, R. A., Sobey, C. G., Stefanska, B., Stephens, G., Teixeira, M., & Ahluwalia, A. (2020). ARRIVE 2.0 and the British Journal of Pharmacology: Updated guidance for 2020. *British Journal of Pharmacology*, *177*(16), 3611–3616. https://doi.org/10.1111/BPH.15178

Lisse, T. S., Elias, L. J., Pellegrini, A. D., Martin, P. B., Spaulding, E. L., Lopes, O., Brochu, E. A., Carter, E. V., Waldron, A., & Rieger, S. (2016). Paclitaxel-induced epithelial damage and ectopic MMP-13 expression promotes neurotoxicity in zebrafish. *Proceedings of the National Academy of Sciences of the United States of America*, *113*, E2189–E2198. https://doi.org/10.1073/pnas.1525096113

Liu, C., Luan, S., OuYang, H., Huang, Z., Wu, S., Ma, C., Wei, J., & Xin, W. (2016). Upregulation of CCL2 via ATF3/c-Jun interaction mediated the Bortezomib-induced peripheral neuropathy. *Brain, Behavior, and Immunity*, *53*, 96–104. https://doi.org/10.1016/j.bbi.2015.11.004

Low, S. E., Ryan, J., Sprague, S. M., Hirata, H., Cui, W. W., Zhou, W., Hume, R. I., Kuwada, J. Y., & Saint-Amant, L. (2010). *touché* is required for touch-evoked generator potentials within vertebrate sensory neurons. *The Journal of Neuroscience*, *30*, 9359–9367. https://doi.org/10.1523/JNEUROSCI.1639-10.2010

Lysko, D. E., & Talbot, W. S. (2022). Unmyelinated sensory neurons use Neuregulin signals to promote myelination of interneurons in the CNS. *Cell Reports*, *41*, 111669. https://doi.org/10.1016/j.celrep.2022.111669

Malafoglia, V., Bryant, B., Raffaeli, W., Giordano, A., & Bellipanni, G. (2013). The zebrafish as a model for nociception studies. *Journal of Cellular Physiology*, *228*, 1956–1966. https://doi.org/10.1002/jcp.24379

Marcotti, A., Fernández-Trillo, J., González, A., Vizcaíno-Escoto, M., Ros-Arlanzón, P., Romero, L., Vela, J. M., Gomis, A., Viana, F., & de la Peña, E. (2023). TRPA1 modulation by Sigma-1 receptor prevents oxaliplatin-induced painful peripheral neuropathy. *Brain*, *146*, 475–491. https://doi.org/10.1093/brain/awac273

Materazzi, S., Fusi, C., Benemei, S., Pedretti, P., Patacchini, R., Nilius, B., Prenen, J., Creminon, C., Geppetti, P., & Nassini, R. (2012). TRPA1 and TRPV4 mediate paclitaxel-induced peripheral neuropathy in mice via a glutathione-sensitive mechanism. *Pflügers Archiv*, *463*, 561–569. https://doi.org/10.1007/s00424-011-1071-x

McGraw, H. F., Nechiporuk, A., & Raible, D. W. (2008). Zebrafish dorsal root ganglia neural precursor cells adopt a glial fate in the absence of neurogenin1. *The Journal of Neuroscience*, *28*, 12558–12569. https://doi.org/10.1523/JNEUROSCI.2079-08.2008

Nassini, R., Gees, M., Harrison, S., De Siena, G., Materazzi, S., Moretto, N., Failli, P., Preti, D., Marchetti, N., Cavazzini, A., Mancini, F., Pedretti, P., Nilius, B., Patacchini, R., & Geppetti, P. (2011). Oxaliplatin elicits mechanical and cold allodynia in rodents via TRPA1 receptor stimulation. *Pain*, *152*, 1621–1631. https://doi.org/10.1016/j.pain.2011.02.051

Nassini, R., Materazzi, S., Benemei, S., & Geppetti, P. (2014). The TRPA1 channel in inflammatory and neuropathic pain and migraine. *Reviews of Physiology, Biochemistry and Pharmacology*, *167*, 1–43. https://doi.org/10.1007/112_2014_18

Ohnesorge, N., Heinl, C., & Lewejohann, L. (2021). Current methods to investigate nociception and pain in zebrafish. *Frontiers in Neuroscience*, *15*, 632634. https://doi.org/10.3389/fnins.2021.632634

Oliveira, J. T., Yanick, C., Wein, N., & Gomez Limia, C. E. (2023). Neuron-Schwann cell interactions in peripheral nervous system homeostasis, disease, and preclinical treatment. *Frontiers in Cellular Neuroscience*, *17*, 1248922. https://doi.org/10.3389/fncel.2023.1248922

Pak, V. V., Ezerina, D., Lyublinskaya, O. G., Pedre, B., Tyurin-Kuzmin, P. A., Mishina, N. M., Thauvin, M., Young, D., Wahni, K., Gache, S. A., &

Demidovich, A. D. (2020). Ultrasensitive genetically encoded indicator for hydrogen peroxide identifies roles for the oxidant in cell migration and mitochondrial function. *Cell Metabolism*, *31*(642–653), e646.

Percie du Sert, N., Hurst, V., Ahluwalia, A., Alam, S., Avey, M. T., Baker, M., Browne, W. J., Clark, A., Cuthill, I. C., Dirnagl, U., Emerson, M., Garner, P., Holgate, S. T., Howells, D. W., Karp, N. A., Lazic, S. E., Lidster, K., MacCallum, C. J., Macleod, M., … Würbel, H. (2020a). The ARRIVE guidelines 2.0: updated guidelines for reporting animal research. *PLoS Biology*, *18*(7), e3000410. https://doi.org/10.1371/journal.pbio.3000410

Peters, C. M., Jimenez-Andrade, J. M., Jonas, B. M., Sevcik, M. A., Koewler, N. J., Ghilardi, J. R., Wong, G. Y., & Mantyh, P. W. (2007). Intravenous paclitaxel administration in the rat induces a peripheral sensory neuropathy characterized by macrophage infiltration and injury to sensory neurons and their supporting cells. *Experimental Neurology*, *203*, 42–54. https://doi.org/10.1016/j.expneurol.2006.07.022

Pietri, T., Manalo, E., Ryan, J., Saint-Amant, L., & Washbourne, P. (2009). Glutamate drives the touch response through a rostral loop in the spinal cord of zebrafish embryos. *Developmental Neurobiology*, *69*, 780–795. https://doi.org/10.1002/dneu.20741

Prober, D. A., Zimmerman, S., Myers, B. R., McDermott, B. M. Jr., Kim, S. H., Caron, S., Rihel, J., Solnica-Krezel, L., Julius, D., Hudspeth, A. J., & Schier, A. F. (2008). Zebrafish TRPA1 channels are required for chemosensation but not for thermosensation or mechanosensory hair cell function. *The Journal of Neuroscience*, *28*, 10102–10110. https://doi.org/10.1523/JNEUROSCI.2740-08.2008

Robinson, C. R., Zhang, H., & Dougherty, P. M. (2014). Astrocytes, but not microglia, are activated in oxaliplatin and bortezomib-induced peripheral neuropathy in the rat. *Neuroscience*, *274*, 308–317. https://doi.org/10.1016/j.neuroscience.2014.05.051

Sawada, Y., Hosokawa, H., Matsumura, K., & Kobayashi, S. (2008). Activation of transient receptor potential ankyrin 1 by hydrogen peroxide. *The European Journal of Neuroscience*, *27*, 1131–1142. https://doi.org/10.1111/j.1460-9568.2008.06093.x

Seretny, M., Currie, G. L., Sena, E. S., Ramnarine, S., Grant, R., MacLeod, M. R., Colvin, L. A., & Fallon, M. (2014). Incidence, prevalence, and predictors of chemotherapy-induced peripheral neuropathy: A systematic review and meta-analysis. *Pain*, *155*, 2461–2470. https://doi.org/10.1016/j.pain.2014.09.020

Shin, Y. K., Jang, S. Y., Lee, H. K., Jung, J., Suh, D. J., Seo, S. Y., & Park, H. T. (2010). Pathological adaptive responses of Schwann cells to endoplasmic reticulum stress in bortezomib-induced peripheral neuropathy. *Glia*, *58*, 1961–1976. https://doi.org/10.1002/glia.21065

Souza Monteiro de Araujo, D., Nassini, R., Geppetti, P., & De Logu, F. (2020). TRPA1 as a therapeutic target for nociceptive pain. *Expert Opinion on Therapeutic Targets*, *24*, 997–1008.

Stevens, J. S., Padilla, S., DeMarini, D. M., Hunter, D. L., Martin, W. K., Thompson, L. C., Gilmour, M. I., Hazari, M. S., & Farraj, A. K. (2018). Zebrafish locomotor responses reveal irritant effects of fine particulate matter extracts and a role for TRPA1. *Toxicological Sciences*, *161*, 290–299. https://doi.org/10.1093/toxsci/kfx217

Takahashi, N., & Mori, Y. (2011). TRP channels as sensors and signal integrators of redox status changes. *Frontiers in Pharmacology*, *2*, 58. https://doi.org/10.3389/fphar.2011.00058

Trevisan, G., Materazzi, S., Fusi, C., Altomare, A., Aldini, G., Lodovici, M., Patacchini, R., Geppetti, P., & Nassini, R. (2013). Novel therapeutic strategy to prevent chemotherapy-induced persistent sensory neuropathy by TRPA1 blockade. *Cancer Research*, *73*, 3120–3131. https://doi.org/10.1158/0008-5472.CAN-12-4370

Trevisani, M., Siemens, J., Materazzi, S., Bautista, D. M., Nassini, R., Campi, B., Imamachi, N., Andrè, E., Patacchini, R., Cottrell, G. S., Gatti, R., Basbaum, A. I., Bunnett, N. W., Julius, D., & Geppetti, P. (2007). 4-Hydroxynonenal, an endogenous aldehyde, causes pain and neurogenic inflammation through activation of the irritant receptor TRPA1. *Proceedings of the National Academy of Sciences of the United States of America*, *104*, 13519–13524. https://doi.org/10.1073/pnas.0705923104

Vallejo, R., Tilley, D. M., Vogel, L., & Benyamin, R. (2010). The role of glia and the immune system in the development and maintenance of neuropathic pain. *Pain Practice*, *10*, 167–184. https://doi.org/10.1111/j.1533-2500.2010.00367.x

Warwick, R. A., & Hanani, M. (2013). The contribution of satellite glial cells to chemotherapy-induced neuropathic pain. *European Journal of Pain*, *17*, 571–580. https://doi.org/10.1002/j.1532-2149.2012.00219.x

Xie, M., Kamenev, D., Kaucka, M., Kastriti, M. E., Zhou, B., Artemov, A. V., Storer, M., Fried, K., Adameyko, I., Dyachuk, V., & Chagin, A. S. (2019). Schwann cell precursors contribute to skeletal formation during embryonic development in mice and zebrafish. *Proceedings of the National Academy of Sciences of the United States of America*, *116*, 15068–15073. https://doi.org/10.1073/pnas.1900038116

Yamamoto, K., Chiba, N., Chiba, T., Kambe, T., Abe, K., Kawakami, K., Utsunomiya, I., & Taguchi, K. (2015). Transient receptor potential ankyrin 1 that is induced in dorsal root ganglion neurons contributes to acute cold hypersensitivity after oxaliplatin administration. *Molecular Pain*, *11*, 69. https://doi.org/10.1186/s12990-015-0072-8

Zajaczkowska, R., Kocot-Kepska, M., Leppert, W., Wrzosek, A., Mika, J., & Wordliczek, J. (2019). Mechanisms of chemotherapy-induced peripheral neuropathy. *International Journal of Molecular Sciences*, *20*, 1451. https://doi.org/10.3390/ijms20061451

Zimmermann, M. (1983). Ethical guidelines for investigations of experimental pain in conscious animals. *Pain*, *16*, 109–110. https://doi.org/10.1016/0304-3959(83)90201-4

SUPPORTING INFORMATION

Additional supporting information can be found online in the Supporting Information section at the end of this article.

How to cite this article: Bellantoni, E., Marini, M., Chieca, M., Gabellini, C., Crapanzano, E. L., Souza Monteiro de Araujo, D., Nosi, D., Roschi, L., Landini, L., De Siena, G., Pensieri, P., Mastricci, A., Scuffi, I., Geppetti, P., Nassini, R., & De Logu, F. (2024). Schwann cell transient receptor potential ankyrin 1 (TRPA1) ortholog in zebrafish larvae mediates chemotherapy-induced peripheral neuropathy. *British Journal of Pharmacology*, 1–15. https://doi.org/10.1111/bph.17318